

NASA Technical Memorandum 107254

Tensile Strength and Microstructural Characterization of Uncoated and Coated HPZ Ceramic Fibers

Narottam P. Bansal and Donald R. Wheeler
Lewis Research Center
Cleveland, Ohio

Robert M. Dickerson
NYMA, Inc.
Brook Park, Ohio

July 1996



National Aeronautics and
Space Administration

Trade names or manufacturers' names are used in this report for identification only. This usage does not constitute an official endorsement, either expressed or implied, by the National Aeronautics and Space Administration.

TENSILE STRENGTH AND MICROSTRUCTURAL CHARACTERIZATION OF UNCOATED AND COATED HPZ CERAMIC FIBERS

Narottam P. Bansal and Donald R. Wheeler
National Aeronautics and Space Administration
Lewis Research Center
Cleveland, Ohio 44135

and

Robert M. Dickerson
NYMA, Inc.
Brook Park, Ohio 44142

SUMMARY

Tensile strengths of as-received HPZ fiber and those surface coated with BN, BN/SiC, and BN/Si₃N₄ have been determined at room temperature using a two-parameter Weibull distribution. Nominally ~0.4 μm BN and 0.2 μm SiC or Si₃N₄ coatings were deposited on the fibers by chemical vapor deposition using a continuous reactor. The average tensile strength of uncoated HPZ fiber was 2.0±0.56 GPa (290±81 ksi) with a Weibull modulus of 4.1. For the BN coated fibers, the average strength and the Weibull modulus increased to 2.39±0.44 GPa (346±64 ksi) and 6.5, respectively. The HPZ/BN/SiC fibers showed an average strength of 2.0±0.32 GPa (290±47 ksi) and Weibull modulus of 7.3. Average strength of the fibers having a dual BN/Si₃N₄ surface coating degraded to 1.15±0.26 GPa (166±38 ksi) with a Weibull modulus of 5.3. The chemical composition and thickness of the fiber coatings were determined using scanning Auger analysis. Microstructural analysis of the fibers and the coatings was carried out by scanning electron microscopy and transmission electron microscopy. A microporous silica-rich layer ~200 nm thick is present on the as-received HPZ fiber surface. The BN coatings on the fibers are amorphous to partly turbostratic and contaminated with carbon and oxygen. Silicon carbide coating was crystalline whereas the silicon nitride coating was amorphous. The silicon carbide and silicon nitride coatings are nonstoichiometric, nonuniform, and granular. Within a fiber tow, the fibers on the outside had thicker and more granular coatings than those on the inside.

1. INTRODUCTION

The HPZ ceramic fiber is an inorganic silicon carbonitride fiber manufactured from hydridopolysilazane polymer via a pyrolytic process by Dow Corning Corporation. It has an oval cross section and is amorphous with a typical elemental composition of 57%Si, 28%N, 10%C, and 4%O. The thermal expansion coefficient of HPZ fiber is ~3×10⁻⁶/°C (ref. 1). It has a desirable combination of tensile strength, elastic modulus, density, and electrical properties and retention of these properties at temperatures up to ~1400 °C (ref. 1), making it suitable for a variety of aerospace applications. It is intended as a reinforcement in high performance composites with ceramic, metal and polymer matrices.

The HPZ fiber surface is microporous and extremely reactive when in contact with aluminosilicate glass-ceramic matrices at high temperatures. According to Brennan (ref. 2), diffusion of matrix elements such as Ba, Mg, Al, Si, and O through this porous surface layer occurs very rapidly, resulting in crystallization of the underlying HPZ fiber to silicon oxynitride, Si₂N₂O. The HPZ fiber surface needs to be protected with appropriate ceramic coating(s) in order to alleviate chemical reactions with ceramic matrices during composite processing and use and also, to provide a weak fiber-matrix interface for toughened composites.

The primary objective of the present study was to investigate the effect of CVD ceramic surface coatings on the strength of the HPZ fiber. This provides a data base for planned work directed at incorporating these coated fibers as reinforcement in celsian matrix composites. Another objective was to carry out microstructural and chemical analyses of the fiber and the coatings. Room temperature tensile strengths of the as-received HPZ fibers and those coated with

BN, BN/SiC, and BN/Si₃N₄ were measured and the Weibull statistical parameters determined for each type of fiber. Elemental compositions and thickness of the fiber coatings were determined by scanning Auger analysis. The microstructural analyses of the fibers and the coatings were done by scanning electron microscopy (SEM) and transmission electron microscopy (TEM).

2. MATERIALS AND EXPERIMENTAL PROCEDURES

The fiber used in the present study was the X9-6371 HPZ ceramic fiber, lot number 031860, having 1000 denier and nominally 500 filaments/tow and supplied by Dow Corning Corporation. The polyvinyl alcohol (PVA) sizing on the fibers was removed either by dipping the fiber bundle in boiling water for several minutes or in a bunsen burner flame. Single filaments were carefully separated from the fiber tow for testing.

All the coatings on the fibers were applied by an outside vendor using a continuous CVD reactor. The BN coating was deposited at ~1000 °C utilizing a proprietary precursor and was amorphous to partly turbostratic in nature. A thin overcoating of SiC or Si₃N₄ was also applied by CVD to the BN-coated fibers. The nominal coating thicknesses were 0.4 μm for BN and 0.2 μm for SiC or Si₃N₄.

2.1 Electron Microscopy

Surfaces of the uncoated and coated loose HPZ fibers were examined using scanning electron microscopy (SEM). For cross-sectional analysis, fibers were mounted in a high temperature epoxy and polished before examination. SEM was performed using a JEOL JSM6100 operating at 15 keV. Fiber cross-sectional thin foils for transmission electron microscopy (TEM) were prepared using a procedure developed for ceramic fibers which involves epoxy potting, slicing, polishing, dimple grinding, and Ar ion beam milling. A thin carbon coating was evaporated onto the thin foils and the SEM specimens for electrical conductivity prior to analysis. The thin foils were examined in a Philips EM400T operating at 120 keV. X-ray elemental analyses on the TEM were acquired using a Kevex thin window energy dispersive spectrometer (EDS) and analyzer.

2.2. Scanning Auger Analysis

The elemental compositions of the fiber near the surface and of the fiber surface coatings were analyzed with a scanning Auger microprobe (Fisons Model 310F). The fibers for this analysis were mounted by pressing into indium foil to minimize electrical charging during analysis. Depth profiling was performed by sequential ion-beam sputtering and Auger analysis. The ion etching was done with an Ar⁺ beam of 3 kV accelerating voltage and beam current of 420 nA and rastered over ~1 mm² area on the specimen. The beam was oriented 48° to the specimen normal and was oblique to the fiber axis. The etch rate in Ta₂O₅ under these conditions was 0.41 nm/s.

AES analysis was performed with the sample normal 60° to the electron beam and parallel to the analyzer axis. The beam was rastered over a 1 μm² area at 100 kX during analysis and centered on the fiber. The beam voltage was 1.5 kV and the beam current was ~5.5 nA. Spectra were taken in integral (as opposed to derivative) form, and depth profiles were created by plotting peak areas against ion etch time. The atomic concentrations were calculated by dividing the peak areas by sensitivity factors derived from spectra of several standard materials containing that element, then scaling the results to total 100 percent. The sensitivity factors used for each element should not be trusted to better than ±20 percent. The depth scale is from the Ta₂O₅ calibration and has not been adjusted for the actual etch rate of the material. Only the fibers with smooth surface coating, rather than those having thick and rough coating morphologies, were used for Auger analysis.

2.3. Tensile Strength Measurement

Room temperature tensile strengths of the individual filaments were measured in ambient atmosphere with an Instron machine (Model # 4502) at a constant crosshead speed of 1.27 mm/min (0.05 in./min). A single filament was mounted on a paper tab with an epoxy. The side portions of the tab were cut with a hot wire just before application of the load producing a fiber gage length of 2.54 cm (1 in.). The fracture pieces were captured by applying a water based

lubricating jelly to the fiber prior to test thus causing the fragments to stick on tissue paper placed behind the test fiber. Twenty filaments of each type of fiber were tested. Some of the HPZ fibers were round but hollow and were not included in strength measurements.

A large variation in the fiber diameter was observed, although the manufacturer reports an average value of ~10 to 12 μm . Because of their oblong shape, the method as shown in figure 1, was used to calculate the cross-sectional area of the fiber following the tensile test. A Zeiss optical microscope at a magnification of 500X was used to measure both the major (D) and the minor (d) diameters at one of the fracture surfaces of the fiber. Possibly, but most likely not, the primary fracture surface was viewed in the microscope. The cross-sectional surface area was calculated from the equation:

$$\begin{aligned}\text{Fiber cross - sectional area} &= \text{Area A} + \text{Area B} + \text{Area C} \\ &= (1/2)\pi(d/2)^2 + (D - d)d + (1/2)\pi(d/2)^2 \\ &= \pi d^2/4 + (D - d)d\end{aligned}\tag{1}$$

3. RESULTS AND DISCUSSION

3.1 Electron Microscopic Analysis

3.1.1 HPZ fiber.—SEM micrographs showing the surface and cross-section of as-received, desized HPZ fibers are given in figures 2 and 3, respectively. The fiber surface is fairly smooth and featureless. The fiber cross-section is oblong with average major and minor diameters of 14.4 and 8.4 μm (“D” and “d” in fig. 1), respectively. It should be noted that the HPZ fibers often crack during the early stages of cross-sectional polishing due to a lack of constraint in the epoxy mounts. A core and rim structure in the fiber cross-section is also revealed. This is even more apparent in the TEM micrograph shown in figure 4. The speckled contrast within the rim region is due to under-focussed imaging conditions used to enhance contrast and is not indicative of the scale of any actual structure. The average thickness of the fiber rim, which is seen to be microporous, was determined to be ~360 nm. Electron micro-diffraction patterns taken from both the core and rim regions (fig. 4 insets) are diffuse rings indicating an amorphous to nanocrystalline crystal structure. EDS compositional spectra taken from the core and rim regions are shown in figure 5. The fiber core is rich in Si and N and contains small amounts of C, O, Al, and Cl. The rim is mostly Si and O, but some C, N, and Al were detected, as well.

3.1.2 HPZ/BN fiber.—An SEM micrograph of a fiber after coating with BN is given as figure 6(a). Cross-sectional micrographs gave poor contrast, due to the low signal yield from the BN, due to its low atomic weight. The coating can spall off from the fibers when broken in bending to reveal multiple layers (fig. 6 (b)). The outermost layer of BN was often quite nodular, as can be seen in figure 6(a) and (b). TEM dark field images of the BN layer revealed a radial structure not visible in bright field images (fig. 7). Microdiffraction patterns from the BN (fig. 7 inset) showed a turbostratic structure.

3.1.3 HPZ/BN/SiC fiber.—The nodules in the BN layer remain or, often, are enhanced by the subsequent coating of SiC (fig. 8). The density of the nodules varies considerably from fiber to fiber, but is more consistent along each individual fiber. The coated nodules are primarily somewhat less than 1 μm in diameter. Sharp contrast is observed between the fiber core, fiber rim, BN coating, and SiC coating in polished cross-sections (fig. 9). The thickness of the outer SiC coating varies from fairly uniform to quite variable and granular. The BN coating thickness varies from approximately 360 to 800 nm between fibers. The SiC coating ranges from about 140 nm to as thick as 5 μm when a granular cluster is attached. Within a tow, the fibers on the outside had thicker and more granular coatings than those on the inside. TEM cross-sections (figs. 10 and 11) reveal the layered structure of the coating. No structural or chemical changes are observed in the fiber cores and rims. A thin band of relatively featureless material is found at the rim/BN interface (fig. 10). This band ion mills more quickly during sample preparation than the surrounding material and might be silica-rich. This region is too narrow to obtain unambiguous crystallographic or compositional information in a conventional TEM, however. Some slight widening of the band is often seen at the tighter radius regions of the fibers, but these regions are usually thinned away during preparation. The BN coating often hints of layering and gives diffraction patterns consistent with a loosely turbostratic structure seen in the as-received fibers. Columnar SiC grains are seen just outside the BN layer. Electron diffraction patterns (fig. 10 inset) indicate that the SiC is crystalline. Diffraction patterns taken from the SiC layers were consistent with a mixture of primarily hexagonal polytypes. The nodular material consists of cores of BN surrounded by columnar SiC (fig. 11). EDS spectra taken from the BN layer

and the nodule cores are quite similar as are the spectra from various sections of the SiC coating. The inner coating was relatively rich in detectable C and N and had some O, Al, and Si. It should be noted that boron is not detectable using the present methods and that some small signals may come from neighboring material. The EDS spectra from the outer layers were those of SiC.

3.1.4 HPZ/BN/Si₃N₄ fiber.—The outer coating on these fibers is also quite granular (fig. 12). More flaws in the smooth underlying Si₃N₄ layer are observed, however. The nodule sizes are very similar to those of the BN/SiC-coated fibers. Outer coating thicknesses vary more widely than the BN/SiC-coated fibers (fig. 13). The clusters attached to some fibers nearly double the fiber dimensions. Several flaws in relatively thin Si₃N₄ layers were observed (arrow in fig. 13(a)). The tows showed similar coating quality and thickness variation as in the BN/SiC coated fibers. Fibers towards the outside of each tow have a thicker and more granular coating than the fibers on the inside. No structural or compositional changes in the fiber rims and cores were detected in the TEM (fig. 14). A thin band of more easily thinned material at the rim/BN interface is seen in these fibers as well. Often, the Si₃N₄ layer was missing completely (fig. 14(a)). The transition from orderly to granular coating structures was often indistinct (fig. 14(b)). While the granules consisted of core and rim structures, the constituents were less distinct crystallographically than the BN/SiC-coated fibers. Compositionally, the BN inner layers and granule cores yielded EDS spectra essentially identical to those of the BN in the BN/SiC-coated fibers. The outer layers are relatively rich in Si and N, as would be expected, and contained more Cl than was found elsewhere. The smooth BN layers were loosely turbostratic while the granule cores gave diffraction ring patterns consistent with nanocrystalline hexagonal BN. The Si₃N₄ layers were not distinctly crystalline as seen from the electron diffraction pattern (fig. 14(b) inset).

3.2. Scanning Auger Analysis

Elemental composition depth profiles, as obtained from scanning Auger analysis, of HPZ fibers and those coated with BN, BN/SiC, and BN/Si₃N₄ are shown in figures 15(a) to (d). The surface of the uncoated HPZ fiber consists of an SiO₂-rich layer having a thickness of ~200 nm. The elemental composition (at %) in the bulk of the fiber is ~49%Si, ~11%C, ~37%N, and ~3%O. The BN layer in the HPZ/BN fiber is ~0.3 μm thick. It may be somewhat rich in boron and is contaminated with ~10 at % of oxygen and ~3 to 5 at % of carbon. At the fiber/coating interface, there is an SiO₂-rich layer about 200 nm thick. The HPZ/BN/SiC fiber has ~150 nm thick layer of Si-rich SiC followed by ~400 nm thick layer of BN. This BN coating appears to be nearly of stoichiometric composition, rather than boron rich, and is much less contaminated with oxygen than the BN layer in HPZ/BN fiber. This is again followed by ~150 nm thick SiO₂-rich layer at the coating/fiber interface. The HPZ/BN/Si₃N₄ fiber has ~300 nm thick layer of Si-rich silicon nitride along with low level contamination of oxygen. This is followed by ~800 nm thick layer of boron-rich BN which is contaminated with ~25 to 30 at % of carbon and ~5 at % of oxygen. A SiO₂-rich layer, ~200 nm thick, is again present at the fiber/coating interface. The thickness of this SiO₂-rich layer, ranging from 0.2 to 1.0 μm, is reported (ref. 6) to vary from fiber to fiber and also from batch to batch of the HPZ fibers, and depends on the fiber processing conditions.

3.3. Tensile Strength

The strength of ceramic fibers is determined by the statistical distribution of flaws in the material. The tensile strength of ceramic fibers is generally analyzed on the basis of the well known Weibull statistics (ref. 7), expressed by the empirical equation:

$$P_s = 1 - P(\sigma) = \exp\left[-V\left\{\frac{\sigma - \sigma_u}{\sigma_0}\right\}^m\right] \quad (2)$$

where P_s is the survival probability ($P(\sigma) = 1 - P_s$ is the failure probability) of an individual fiber at an applied stress of σ , V is the fiber volume, σ_u is the stress below which failure never occurs, σ_0 is the scale parameter, and m is the shape or flaw dispersion parameter. m and σ_0 are constant for a given material. Assuming $\sigma_u = 0$ and uniform fiber diameter along the length L corresponding to the volume V , eq. (2) can be rearranged as:

$$\ln \ln(1/P_s) = \ln \ln[1/(1 - P(\sigma))] = m \ln \sigma + \text{constant} \quad (3)$$

The experimental data can be ranked in ascending order of strength values and the cumulative probability $P(\sigma_i)$ can be assigned as

$$P(\sigma_i) = i/(1 + N) \quad (4)$$

where i is the rank of the tested fiber in the ranked strength tabulation and N is the total number of fibers tested. A least-squares linear regression analysis can then be applied to a plot of $[\ln \ln(1/P_s)]$ vs. $\ln(\sigma)$. The slope of this analysis is the Weibull modulus m . The median strength of the fiber, $\sigma_{0.5}$ (corresponding to $P_s = 0.5$), depends on its length L and is expressed by the expression:

$$\ln \sigma_{0.5} = -(1/m) \ln L + \text{constant} \quad (5)$$

According to eq. (5), a plot of $\ln \sigma_{0.5}$ vs. $\ln L$ should be linear with a slope of $-1/m$.

The $\ln \ln(1/P_s)$ vs. $\ln \sigma$ Weibull probability plots for room temperature tensile strength of uncoated HPZ fibers and those having surface coatings of BN, or BN/SiC are shown in figure 16. Similar Weibull probability plot for BN/Si₃N₄ coated HPZ fibers is given in figure 17. Values of Weibull parameters obtained from linear regression analysis for HPZ fibers with different coatings are given in table I. The average tensile strength of as-received (after sizing removal) HPZ fiber is 2.0 ± 0.56 GPa (290 ± 81 ksi) and the value of m is 4.1. The manufacturer's information data sheet (ref. 1) reports values of 1.72 to 2.07 GPa (250 to 300 ksi) for the room temperature tensile strength of these fibers. Similar strength values of HPZ fibers have also been reported by Takeda et al. (ref. 3). However, Villalobos et al. (ref. 4) report tensile strengths of 1.5 to 1.8 GPa for two different batches of HPZ fibers where as Moorehead and Kim (ref. 5) give 2.83 ± 0.87 GPa as the room temperature tensile strength of these fibers. The BN-coated fibers showed an increase in average tensile strength as well as Weibull modulus to 2.39 ± 0.44 GPa (346 ± 64 ksi) and 6.5, respectively. This may be due to the elimination of fiber surface flaws by the smooth BN coating. The HPZ/BN/SiC fibers showed the same average strength, 2.0 ± 0.32 GPa (290 ± 47 ksi), as the as-received fibers, but the value of m increased to 7.3. The average tensile strength of the BN-Si₃N₄ coated fibers degraded to 1.15 ± 0.26 GPa (166 ± 38 ksi), yet showed an m value of 5.3. Since the BN coating on HPZ fibers resulted in an increase in tensile strength, the reduction in strength of the fibers having dual coatings is probably due to exposure of the BN-coated fibers to high temperatures during chemical vapor deposition of silicon carbide and silicon nitride or to large flaws in these layers. However, it is difficult to guess the exact temperatures experienced by these fibers during CVD as the experimental conditions used during coating of the fibers are considered to be proprietary and were not provided by the vendor. Room temperature tensile strength of the HPZ fibers is known (ref. 5) to degrade after exposure to temperatures as low as 1000 °C for a few hours in air or argon atmospheres.

4. SUMMARY

Room temperature tensile strengths of as-received HPZ fiber and those surface coated with BN, BN/SiC, or BN/Si₃N₄ by CVD have been measured. The uncoated HPZ fiber showed an average tensile strength of 2.0 ± 0.56 GPa (290 ± 81 ksi) and the Weibull modulus of 4.1. For the BN coated fibers, the average strength and the Weibull modulus increased to 2.39 ± 0.44 GPa (346 ± 64 ksi) and 6.5, respectively. The HPZ/BN/SiC fibers showed an average strength of 2.0 ± 0.32 GPa (290 ± 47 ksi) and Weibull modulus of 7.3. The average strength of fibers having dual BN/Si₃N₄ surface coating degraded to 1.15 ± 0.26 GPa (166 ± 38 ksi) with a Weibull modulus of 5.3. Chemical compositions of HPZ fiber and the surface coatings have been determined using scanning Auger analysis. Scanning electron microscopy and transmission electron microscopy were used for microstructural analysis of the fibers and the coatings. A microporous silica-rich layer, ~200 nm thick, is present on the HPZ fiber surface. The BN coatings are amorphous to partly turbostratic and contaminated with carbon and oxygen. Silicon carbide coating was crystalline whereas the silicon nitride coating was amorphous. Silicon carbide and silicon nitride coatings are non-stoichiometric, nonuniform and flaky. Within a fiber tow, the fibers on the outside had thicker and more granular coatings than those on the inside.

5. CONCLUSIONS AND FUTURE WORK

It may be concluded that because of low tensile strength of BN/Si₃N₄ coated HPZ fibers, ceramic matrix composites reinforced with these fibers will not exhibit high strengths. Barium aluminosilicate glass-ceramic matrix composites

reinforced with uncoated and coated HPZ fibers have been fabricated. Measurement of their mechanical properties at room and elevated temperatures is in progress. The fiber/matrix interface and the microstructures of these composites are also being investigated. The results of these findings will be reported in the near future.

ACKNOWLEDGMENTS

Thanks are due to Dr. Frank Honey for the scanning Auger analysis and to Greg Selover for his assistance with the tensile strength measurements.

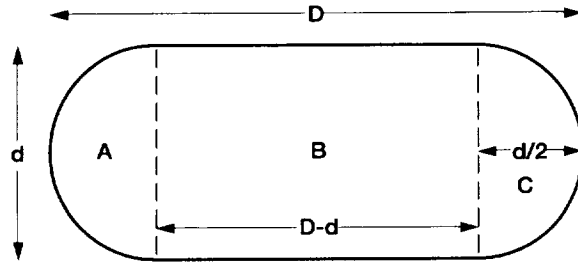
REFERENCES

1. Dow Corning (R) X9-6371 C-2 Sized HPZ Ceramic Fiber Test Report Sheet, May 17, 1991.
2. Brennan, J.J., Interfaces in BN Coated Fiber Reinforced Glass-Ceramic Matrix Composites, *Scr. Met. Mater.*, 31[8], pp. 959-964 (1994).
3. Takeda, M., Imai, Y., Ishikawa, T., Kasai, N., Seguchi, T., and Okamura, K., Thermomechanical Analysis of the Low Oxygen Silicon Carbide Fibers Derived from Polycarbosilane, *Ceram. Eng. Sci. Proc.*, 14[7-8], pp. 540-547 (1993).
4. Villalobos, G.R., Starr, T.L., Piotrowski, D.P., and Sleboda, T.J., Advanced Dielectric Fiber Properties, *Ceram. Eng. Sci. Proc.*, 14[7-8], pp. 682-689 (1993).
5. Moorhead, A.J. and Kim, H.-E., Strength of SiC- and Si-N-C-Ceramic Fibers Exposed to High-Temperature Gaseous Environments, in "Composites: Design, Manufacture, and Application," S.W. Tsai and G.S. Springer, Eds., *Proc. 8th Int. Confr. Comp. Mater. (ICCM/VIII)*, SAMPE, pp. 23D1-23D11 (1991).
6. Zangvil, A., Chang, Y.-W., Finnegan, N., and Lipowitz, J., Effect of Heat Treatment on the Elemental Distribution of Si, C, N, O Fibers, *Ceram. Int.*, 18[4], pp. 271-277 (1992).
7. Weibull, W., A Statistical Distribution Function of Wide Applicability, *J. Appl. Mech.*, 18[9], pp. 293-297 (1951).

TABLE I.—WEIBULL PARAMETERS FOR ROOM TEMPERATURE TENSILE STRENGTHS^a OF UNCOATED AND COATED HPZ FIBERS

Fiber coating	Average strength GPa (ksi)	Weibull modulus m	σ_0 GPa	50 percent survival strength GPa (ksi)
None	2.0±0.56 (290±81)	4.1	2.21	2.02 (293)
BN	2.39±0.44 (346±64)	6.5	2.56	2.42 (351)
BN-SiC	2.0±0.32 (290±47)	7.3	2.13	2.03 (294)
BN-Si ₃ N ₄	1.15±0.26 (166±38)	5.3	1.25	1.16 (169)

^aFor 1 in. test gage length.



$$\begin{aligned}
 \text{Cross-sectional area} &= A + B + C \\
 &= \frac{\pi}{2} (d/2)^2 + (D-d)d + \frac{\pi}{2} (d/2)^2 \\
 &= \frac{\pi d^2}{4} + \frac{D-d}{d}
 \end{aligned}$$

Figure 1.—Calculation of cross-sectional area of HPZ fiber.

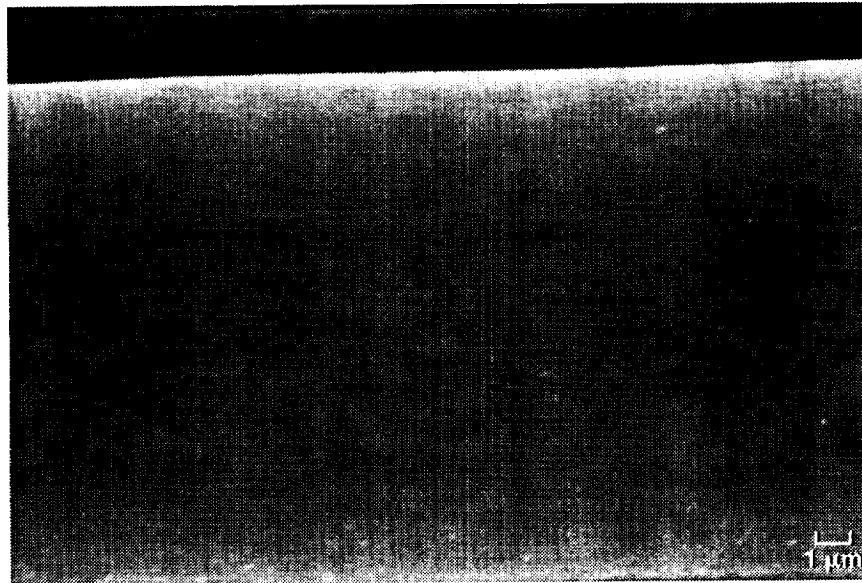


Figure 2.—SEM secondary electron micrograph showing surface of desized HPZ fiber.



Figure 3.—SEM backscattered electron micrograph showing polished cross-section of desized HPZ fiber.

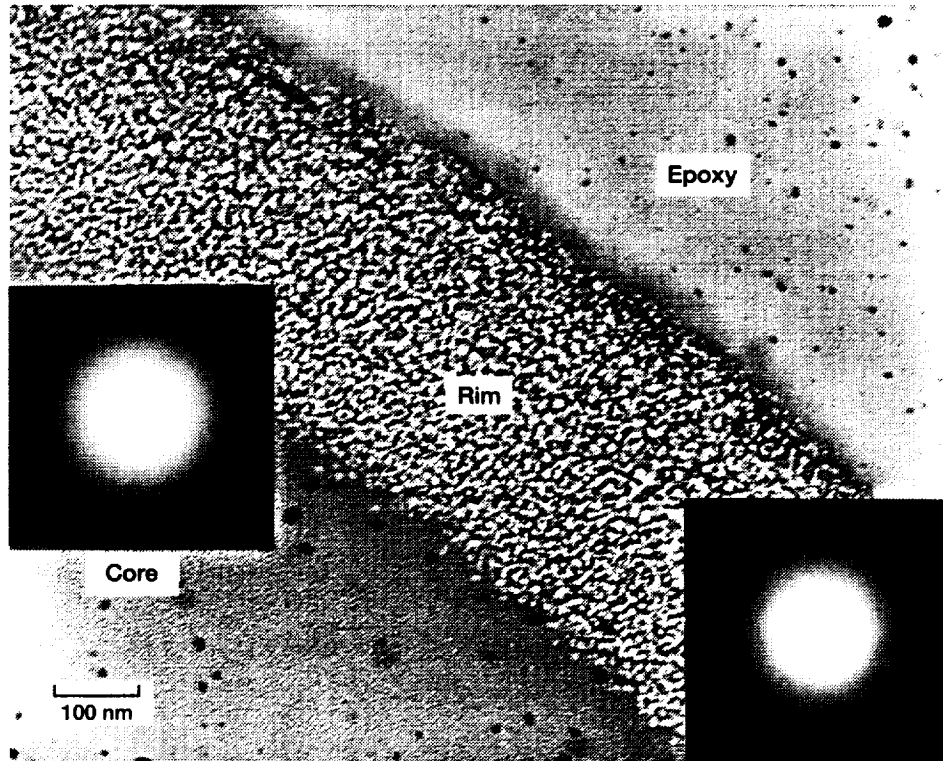


Figure 4.—TEM bright field image of HPZ fiber core and rim in cross-section. Electron micro-diffraction patterns from the core (left) and rim (right) are inset.

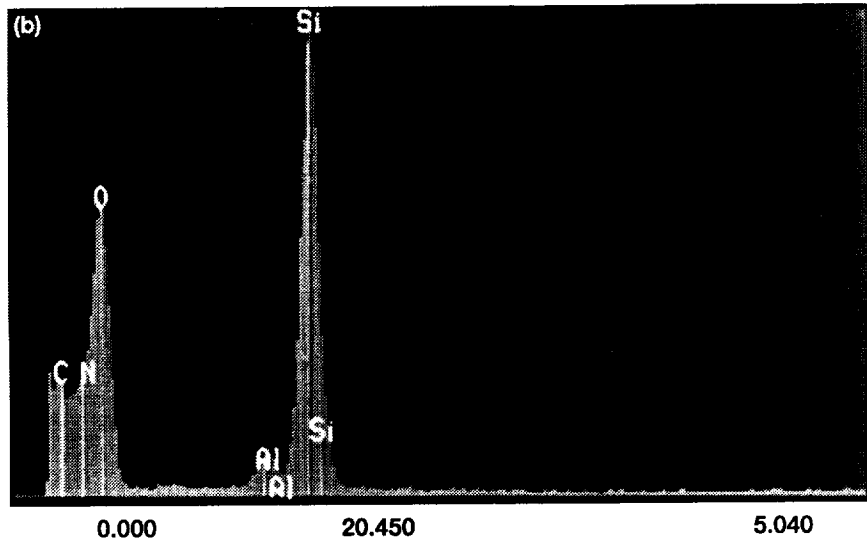
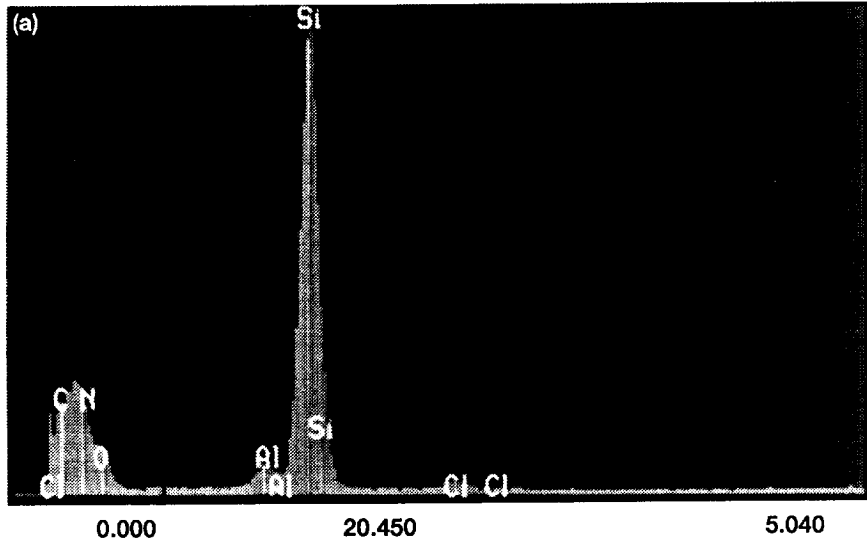


Figure 5.—SEM EDS spectra of HPZ fiber polished cross-section. (a) Fiber core. (b) Rim.

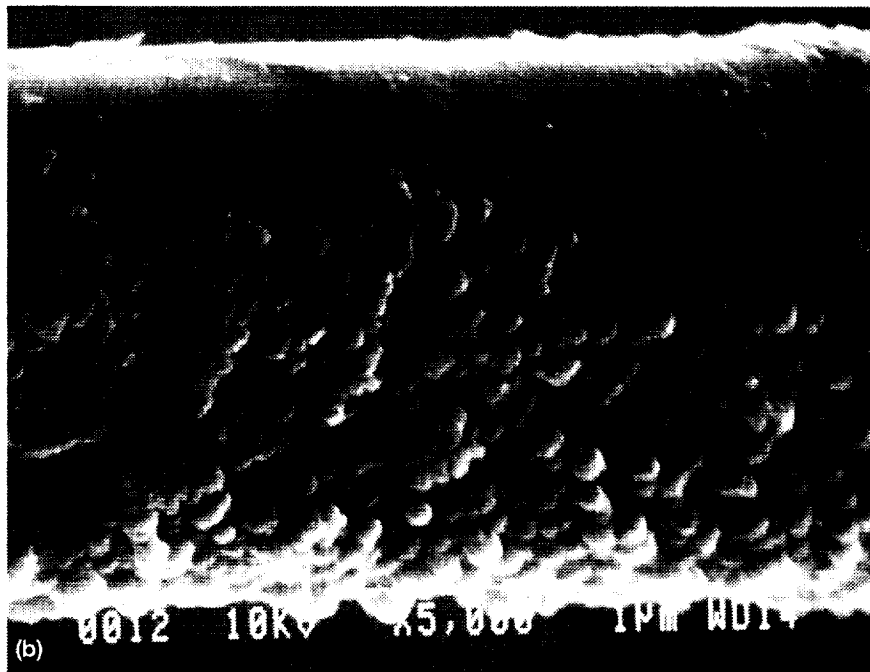
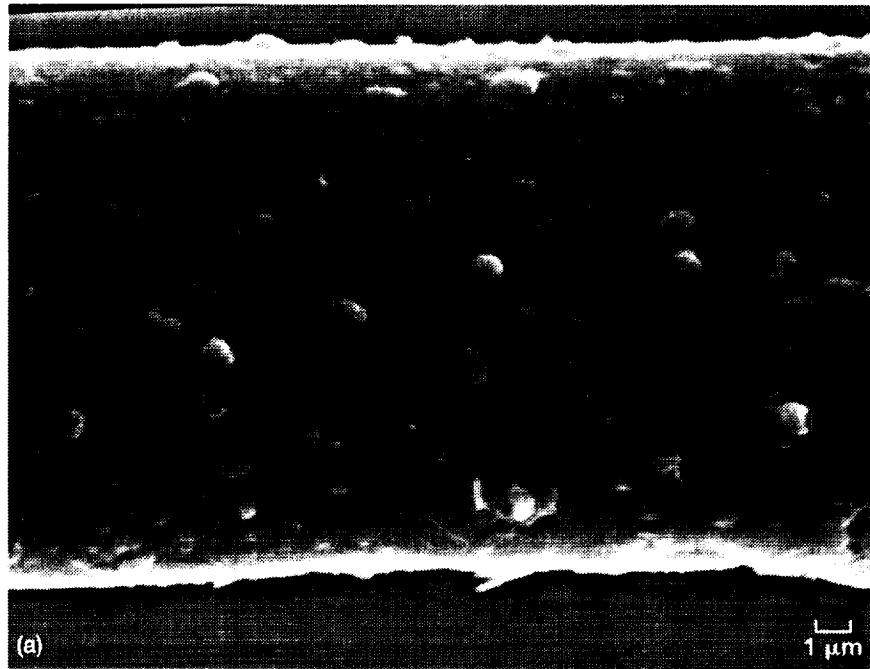


Figure 6.—SEM secondary electron micrograph of HPZ fiber with BN coating.
(a) Viewed from the side. (b) Showing layering.

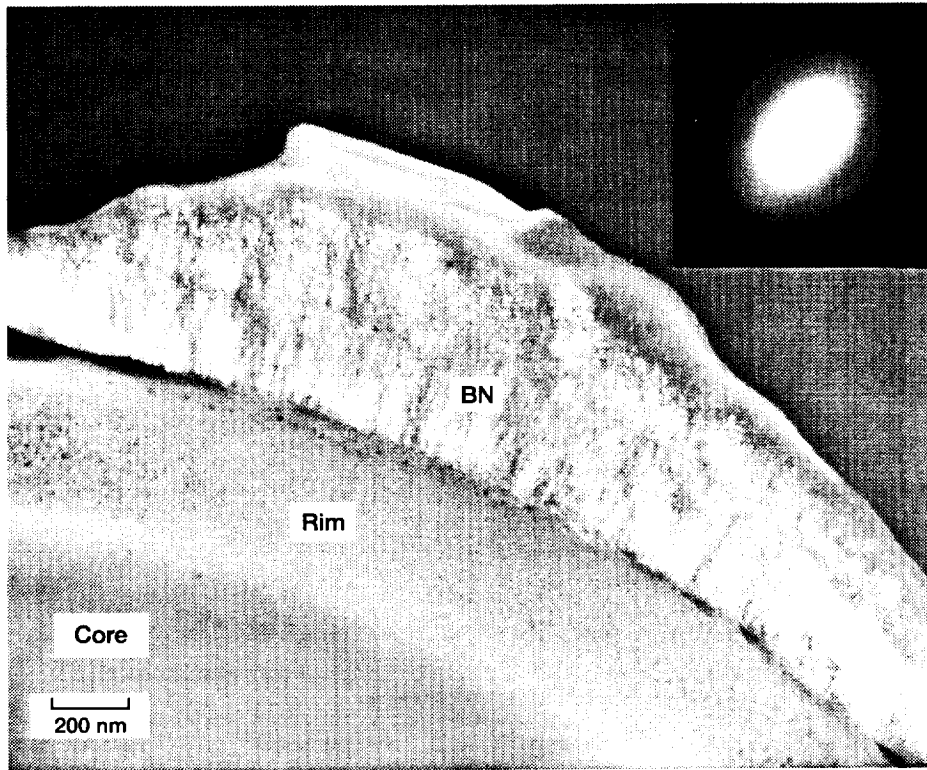


Figure 7.—TEM dark field image of HPZ fiber with BN coating in cross-section. Electron micro-diffraction pattern showing turbostratic structure in the BN is inset.

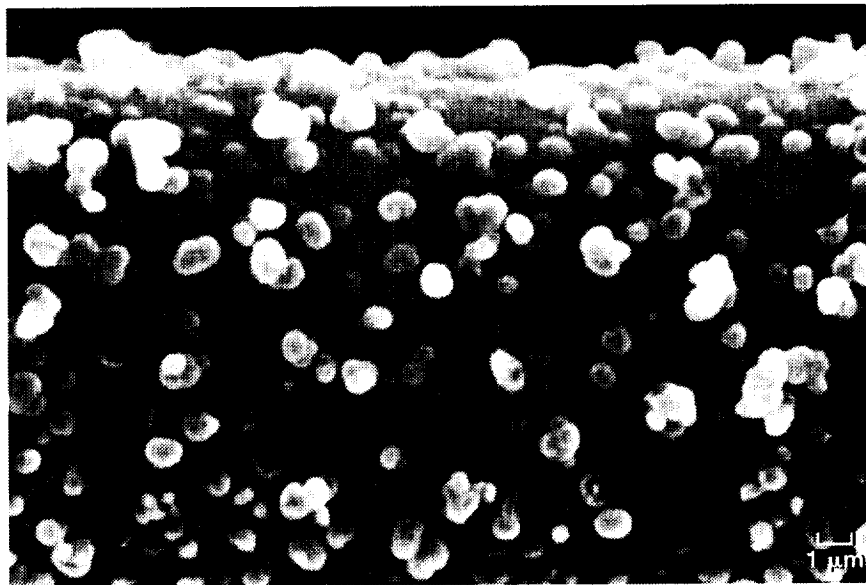


Figure 8.—SEM secondary electron micrograph of HPZ fiber with BN and SiC coatings viewed from the side.

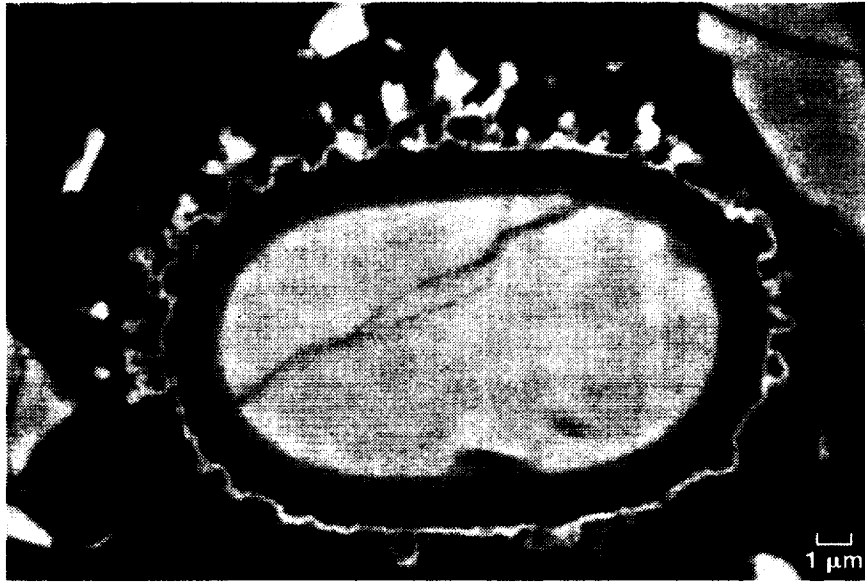


Figure 9.—SEM backscattered electron micrograph showing polished cross-section of HPZ fiber with BN and SiC coatings.

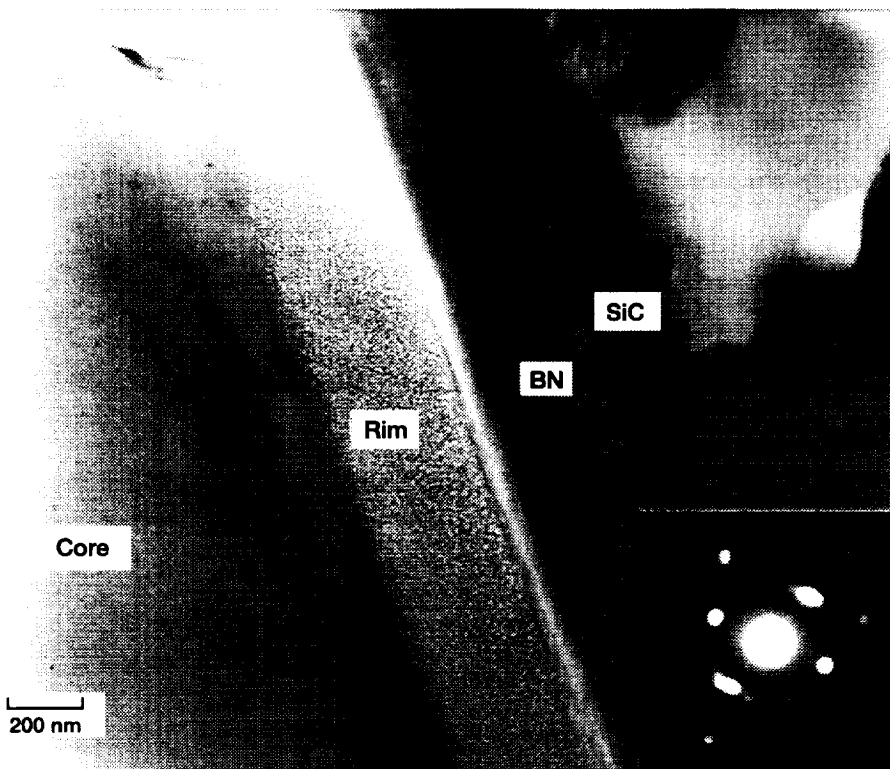


Figure 10.—TEM bright field image of HPZ fiber core and rim and BN and SiC coatings in cross-section. Electron micro-diffraction pattern from the SiC coating is inset.

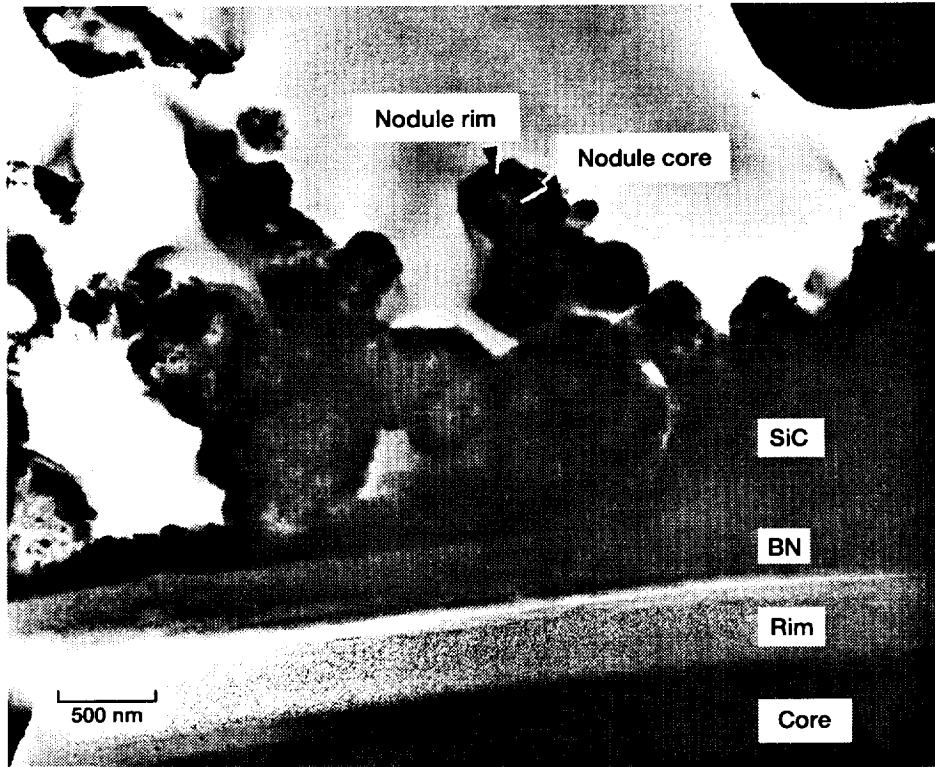


Figure 11.—TEM bright field image of HPZ fiber with BN and SiC coatings in cross-section showing nodular core and rim structure.

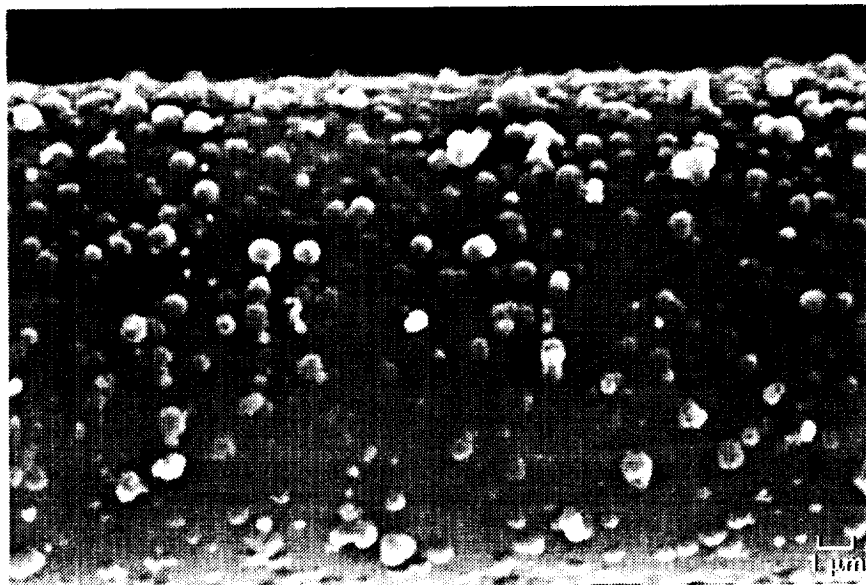


Figure 12.—SEM secondary electron micrograph of HPZ fiber with BN and Si₃N₄ coatings viewed from the side.

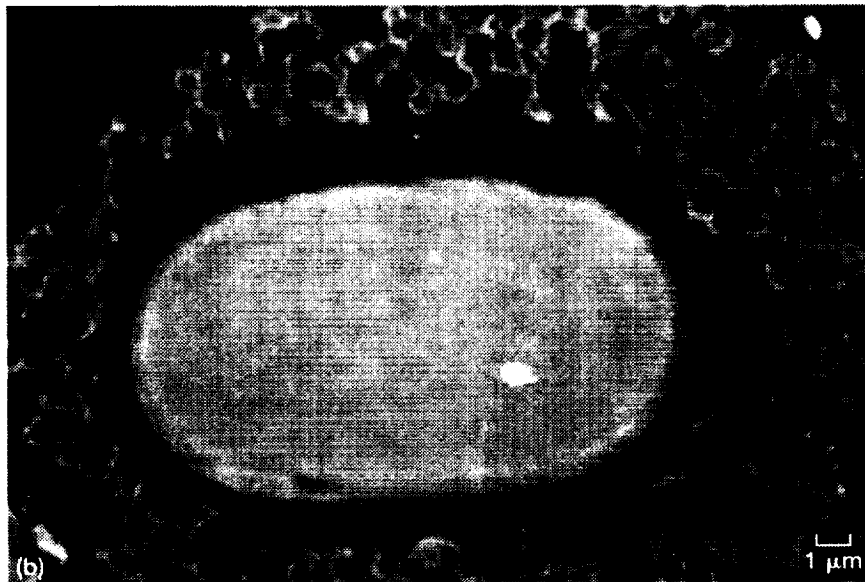
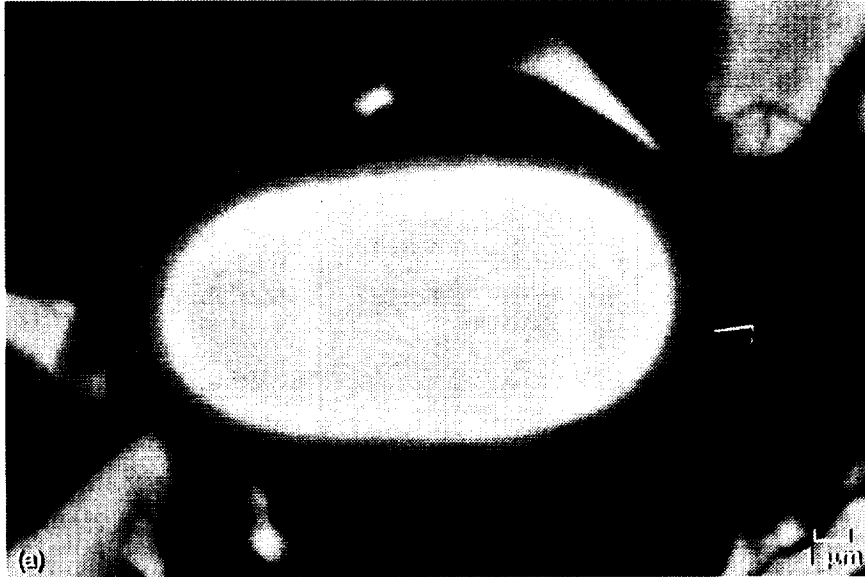


Figure 13.—SEM backscattered electron micrograph of HPZ fiber with BN and Si_3N_4 coatings viewed in polished cross-section. (a) Showing thin coating. (b) Showing thick, granular coating.

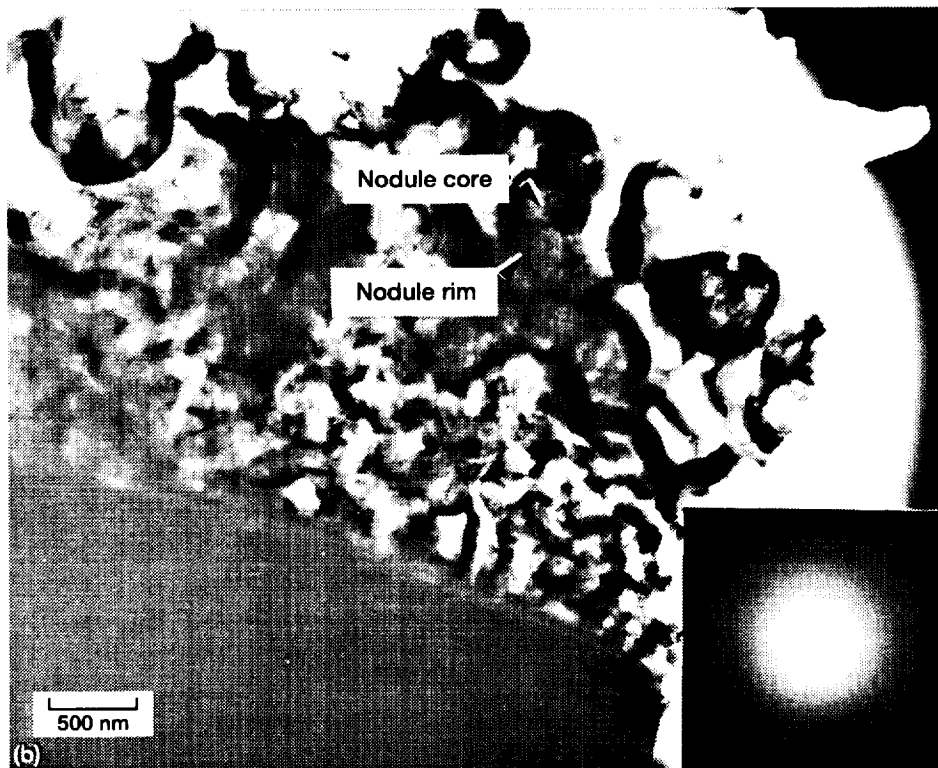
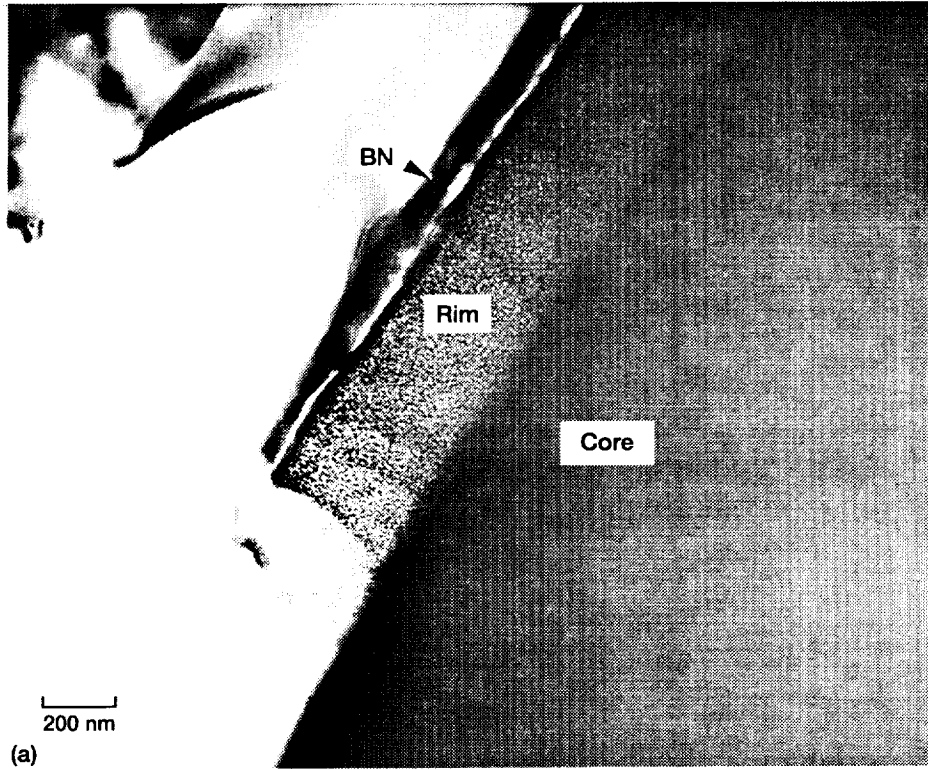


Figure 14.—TEM bright field image of HPZ fiber with BN and Si_3N_4 coatings in cross-section. (a) Si_3N_4 coating is missing. (b) Showing nodular core and rim structure; micro-diffraction pattern from the Si_3N_4 is inset.

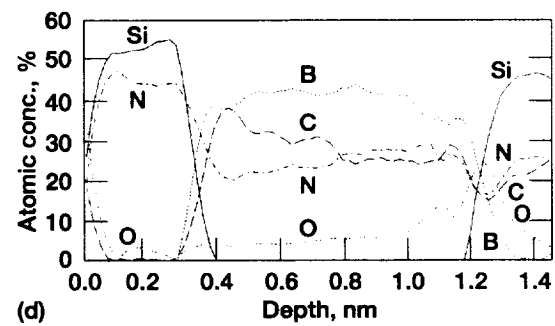
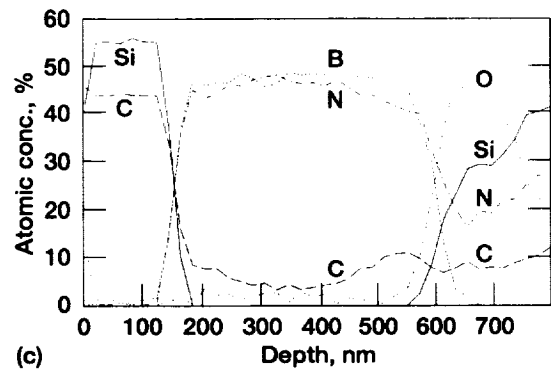
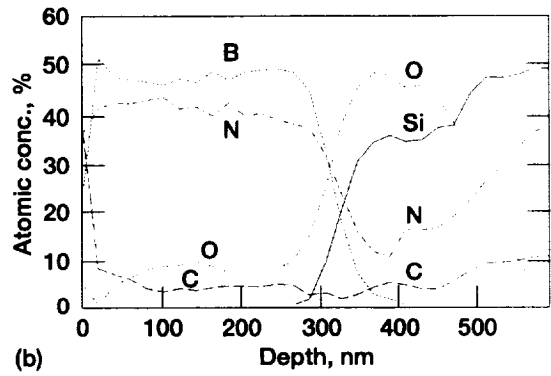
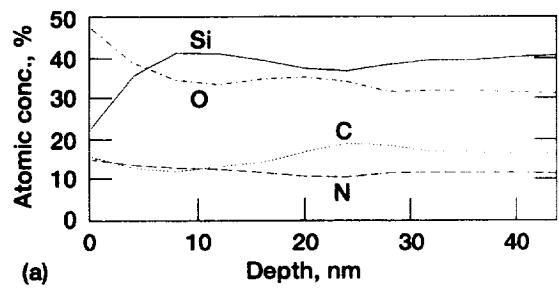


Figure 15.—Depth profiles of various elements.
 (a) HPZ. (b) HPZ/BN. (c) HPZ/BN/SiC.
 (d) HPZ/BN/Si₃N₄ fibers obtained from scanning Auger microprobe.

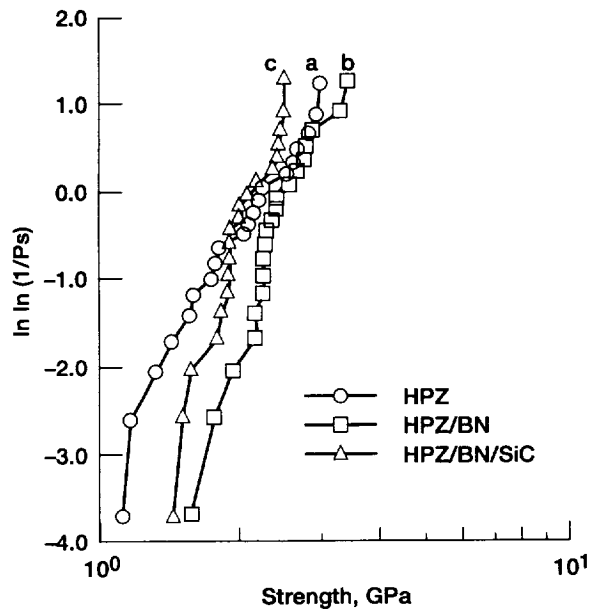


Figure 16.—Weibull probability plot for room temperature tensile strengths. (a) HPZ. (b) HPZ/BN. (c) HPZ/BN/SiC fibers.

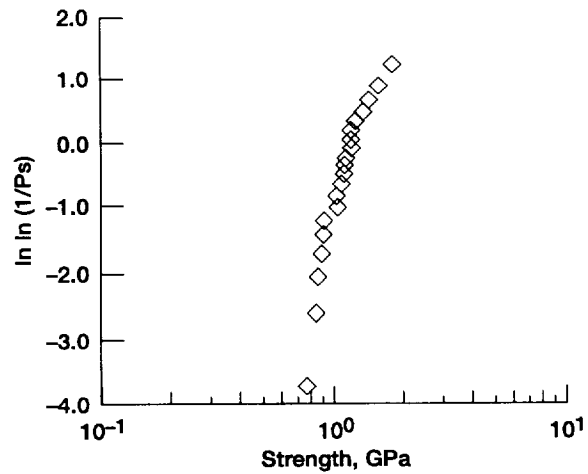


Figure 17.—Weibull probability plot for room temperature tensile strength of HPZ/BN/Si₃N₄ fiber.

REPORT DOCUMENTATION PAGE

Form Approved
OMB No. 0704-0188

Public reporting burden for this collection of information is estimated to average 1 hour per response, including the time for reviewing instructions, searching existing data sources, gathering and maintaining the data needed, and completing and reviewing the collection of information. Send comments regarding this burden estimate or any other aspect of this collection of information, including suggestions for reducing this burden, to Washington Headquarters Services, Directorate for Information Operations and Reports, 1215 Jefferson Davis Highway, Suite 1204, Arlington, VA 22202-4302, and to the Office of Management and Budget, Paperwork Reduction Project (0704-0188), Washington, DC 20503.

1. AGENCY USE ONLY (Leave blank)		2. REPORT DATE July 1996	3. REPORT TYPE AND DATES COVERED Technical Memorandum	
4. TITLE AND SUBTITLE Tensile Strength and Microstructural Characterization of Uncoated and Coated HPZ Ceramic Fibers			5. FUNDING NUMBERS WU-505-63-12	
6. AUTHOR(S) Narottam P. Bansal, Donald R. Wheeler, and Robert M. Dickerson				
7. PERFORMING ORGANIZATION NAME(S) AND ADDRESS(ES) National Aeronautics and Space Administration Lewis Research Center Cleveland, Ohio 44135-3191			8. PERFORMING ORGANIZATION REPORT NUMBER E-10312	
9. SPONSORING/MONITORING AGENCY NAME(S) AND ADDRESS(ES) National Aeronautics and Space Administration Washington, D.C. 20546-0001			10. SPONSORING/MONITORING AGENCY REPORT NUMBER NASA TM-107254	
11. SUPPLEMENTARY NOTES Narottam P. Bansal and Donald R. Wheeler, NASA Lewis Research Center; Robert M. Dickerson, NYMA, Inc., 2001 Aerospace Parkway, Brook Park, Ohio 44142 (work funded by NASA Contract NAS3-27186). Responsible person, Narottam P. Bansal, organization code 5130, (216) 433-3855.				
12a. DISTRIBUTION/AVAILABILITY STATEMENT Unclassified - Unlimited Subject Category 27 This publication is available from the NASA Center for AeroSpace Information, (301) 621-0390.			12b. DISTRIBUTION CODE	
13. ABSTRACT (Maximum 200 words) Tensile strengths of as-received HPZ fiber and those surface coated with BN, BN/SiC, and BN/Si ₃ N ₄ have been determined at room temperature using a two-parameter Weibull distribution. Nominally ~0.4 μm BN and 0.2 μm SiC or Si ₃ N ₄ coatings were deposited on the fibers by chemical vapor deposition using a continuous reactor. The average tensile strength of uncoated HPZ fiber was 2.0 ± 0.56 GPa (290 ± 81 ksi) with a Weibull modulus of 4.1. For the BN coated fibers, the average strength and the Weibull modulus increased to 2.39 ± 0.44 GPa (346 ± 64 ksi) and 6.5, respectively. The HPZ/BN/SiC fibers showed an average strength of 2.0 ± 0.32 GPa (290 ± 47 ksi) and Weibull modulus of 7.3. Average strength of the fibers having a dual BN/Si ₃ N ₄ surface coating degraded to 1.15 ± 0.26 GPa (166 ± 38 ksi) with a Weibull modulus of 5.3. The chemical composition and thickness of the fiber coatings were determined using scanning Auger analysis. Microstructural analysis of the fibers and the coatings was carried out by scanning electron microscopy and transmission electron microscopy. A microporous silica-rich layer ~200 nm thick is present on the as-received HPZ fiber surface. The BN coatings on the fibers are amorphous to partly turbostratic and contaminated with carbon and oxygen. Silicon carbide coating was crystalline whereas the silicon nitride coating was amorphous. The silicon carbide and silicon nitride coatings are non-stoichiometric, non-uniform, and granular. Within a fiber tow, the fibers on the outside had thicker and more granular coatings than those on the inside.				
14. SUBJECT TERMS Tensile strength; HPZ fiber; Electron microscopy; Scanning Auger analysis; Coatings			15. NUMBER OF PAGES 20	
			16. PRICE CODE A03	
17. SECURITY CLASSIFICATION OF REPORT Unclassified	18. SECURITY CLASSIFICATION OF THIS PAGE Unclassified	19. SECURITY CLASSIFICATION OF ABSTRACT Unclassified	20. LIMITATION OF ABSTRACT	